Rapid Climatic Signal Propagation from Source to Sink in a Southern California Sediment-Routing System

Jacob A. Covault, Brian W. Romans, Andrea Fildani, Mary McGann,[1] *and Stephan A. Graham*[2]

Chevron Energy Technology Company, Clastic Stratigraphy R & D, San Ramon, California 94583, U.S.A. (e-mail: jcovault@chevron.com)

ABSTRACT

Terrestrial source areas are linked to deep-sea basins by sediment-routing systems, which only recently have been studied with a holistic approach focused on terrestrial and submarine components and their interactions. Here we compare an extensive piston-core and radiocarbon-age data set from offshore southern California to contemporaneous Holocene climate proxies in order to test the hypothesis that climatic signals are rapidly propagated from source to sink in a spatially restricted sediment-routing system that includes the Santa Ana River drainage basin and the Newport deep-sea depositional system. Sediment cores demonstrate that variability in rates of Holocene deep-sea turbidite deposition is related to complex ocean-atmosphere interactions, including enhanced magnitude and frequency of the North American monsoon and El Niño–Southern Oscillation cycles, which increased precipitation and fluvial discharge in southern California. This relationship is evident because, unlike many sediment-routing systems, the Newport submarine canyon-and-channel system was consistently linked to the Santa Ana River, which maintained sediment delivery even during Holocene marine transgression and highstand. Results of this study demonstrate the efficiency of sediment transport and delivery through a spatially restricted, consistently linked routing system and the potential utility of deep-sea turbidite depositional trends as paleoclimate proxies in such settings.

Introduction

Submarine fans comprise sediment–gravity flow deposits at the terminus of sediment-routing systems in the deep sea, and as such, they generally represent the final resting places of terrigenous sediment (Menard 1955; Normark 1970; Allen 1997, 2008*a*). Therefore, deep-sea deposits often contain relatively complete records of sediment flux from land to sea (Einsele et al. 1996; Romans et al. 2009). However, sediment can be sequestered en route to a deep-sea basin in accommodation along the routing system (e.g., rivers, flood plains, estuaries, subsiding deltas), thereby potentially introducing significant lag time between onshore forcings and offshore deposition (Milliman and Syvitski 1992; Allen 2007, 2008*a*). This is common in extensive sediment-routing systems that drain large proportions of continents, in which the lag time might exceed millions of years (Milliman and Syvitski 1992; Métivier and Gaudemer 1999; Castelltort and Van Den Dreissche 2003). As a result, climatic signals recorded in terrestrial-derived proxies (e.g., tree rings, pollen; Stokstad 2001) might not be faithfully reflected by contemporaneous deep-sea fan deposition.

Here we compare an extensive piston-core and radiocarbon-age data set from the latest Pleistocene-to-Holocene Newport deep-sea depositional system offshore southern California to contemporaneous high-resolution paleoclimate data. Unlike many deep-sea systems, particularly those of passive continental margins with extensive sediment-routing systems and broad shelves (Posamentier et al. 1991), the smaller Newport canyon-and-channel system actively delivered sediment to the fan during the Holocene marine transgression and highstand (cf. Piper and Normark 2001; Covault et al. 2007; Normark et al. 2009; Romans et al. 2009). Therefore, the spatially restricted southern Cali-

Manuscript received September 1, 2009; accepted January 25, 2010.

[1] U.S. Geological Survey, Coastal and Marine Geology Team, Menlo Park, California 94025, U.S.A.

[2] Department of Geological and Environmental Sciences, Stanford University, Stanford, California 94305, U.S.A.

[The Journal of Geology, 2010, volume 118, p. 247–259] 0022-1376/2010/11803-0002$15.00. DOI: 10.1086/651539

fornia sediment-routing system of this study, including the offshore Newport deep-sea depositional system and the onshore Santa Ana River drainage basin, is an ideal natural laboratory in which to assess the efficiency of climatic signal propagation and to demonstrate the utility of deep-sea fan deposits as a paleoclimate proxy resource (cf. Figueiredo et al. 2009). This study represents an early step toward the development of more holistic models of sedimentary systems, including terrestrial and submarine components and their interactions, and it highlights the need for additional, highly temporally resolved studies of large and small sediment-routing systems.

Southern California Sediment-Routing System and Holocene Climate

The southern California sediment-routing system of this study includes the onshore Santa Ana River watershed, which drains steep, tectonically active terrain of the Peninsular Ranges and the San Gabriel and San Bernardino mountains of the Transverse Ranges and the Newport deep-sea depositional system of the California borderland (Normark et al. 2009; fig. 1). The California borderland is the tectonically active region offshore southern California characterized by a relatively narrow shelf and complex basin-and-ridge bathymetry (Shepard and Emery 1941; Ryan et al. 2009). The Newport deep-sea system includes a tributary network of canyons and channels that coalesce at ~600 m below present sea level (m bpsl) in the Gulf of Santa Catalina, which is a basin of the inner (i.e., landward) segment of the borderland (Normark et al. 2009; fig. 1). The Newport channel exhibits a serpentine morphology around prominent knolls, and it spills into a seaward basin at ~800 m bpsl (fig. 1). Normark et al. (2009) indicated that the Newport canyon-and-channel system is longer (~130 km) than other systems on the seafloor of the borderland. Today, a single canyon head of the Newport tributary network is connected to the Santa Ana River mouth (Warrick and Milliman 2003; Normark et al. 2009; fig. 1). Normark et al. (2009) interpreted that this single canyon received sediment from fluvial effluents and mass-wasting processes in the canyon and steep outer shelf during the Holocene marine transgression and highstand based on lack of hemipelagic sediment draping the canyon floor and U.S. Geological Survey piston cores containing recently deposited turbidites (Normark et al. 2009). The contribution and timing of fluvial effluents relative to mass-wasting processes in the canyon and steep outer shelf to the initiation of sediment gravity flows in the Newport system are unknown. However, it is likely that a variety of sediment-gravity-flow initiation mechanisms—from earthquakes associated with the tectonically active borderland setting to hyperpycnal sediment-laden fluvial effluents and deltaic sediment buildup and failure—contributed to the excavation of Newport Canyon (cf. Normark et al. 2009; Piper and Normark 2009; Romans et al. 2009).

The sediment flux from the Santa Ana River is among the largest fluxes reported for semiarid southern California rivers measured during the twentieth century, during which time its discharge achieved hyperpycnal concentrations of suspended sediment during El Niño–Southern Oscillation (ENSO)-induced flood events (Warrick and Milliman 2003). The steep terrain of the Santa Ana River drainage basin predominantly includes relatively resistant Jurassic and Cretaceous plutonic rocks of the Peninsular Ranges and the relatively unconsolidated Tertiary and Quaternary sediment and sedimentary rocks of the Transverse Ranges (Inman and Jenkins 1999). The Newport Canyon head also receives a relatively small proportion of sediment from longshore currents of the San Pedro littoral cell (Masters 2006; Normark et al. 2009; fig. 1).

Southern California climate has been directly monitored since the nineteenth century, a time period too brief to provide an understanding of climatic variability and forcing mechanisms over millennial durations. Proxy measurements from lake sediment are commonly employed in order to reconstruct climate of the more distant past, such as the Holocene epoch (Stokstad 2001). However, local lake conditions can limit the applicability of such proxy records across a broad geographic area (Verschuren 2003). Climate proxies, including magnetic susceptibility, HCl-extractable Al, total inorganic P, total organic matter, and $CaCO_3$ percentage, from drill cores in Lake Elsinore of the relatively small San Jacinto River drainage basin (<1,240 km^2; fig. 1) provide the first complete Holocene record of terrestrial climate in southern California (Kirby et al. 2007; fig. 2). Figure 2 shows plots of these climate proxy measurements, which Kirby et al. (2007) interpreted to represent onshore southern California variability in precipitation and sediment flux since 9.5 ka (see also Kirby et al. 2004). These, and other, proxy measurements were rigorously quantified in order to make qualitative, relative estimates of paleoclimate (Kirby et al. 2007). Therefore, precise numbers of climatic variability, such as precipitation or fluvial discharge, are not available. There is a plethora of information available for twentieth-century precipitation and

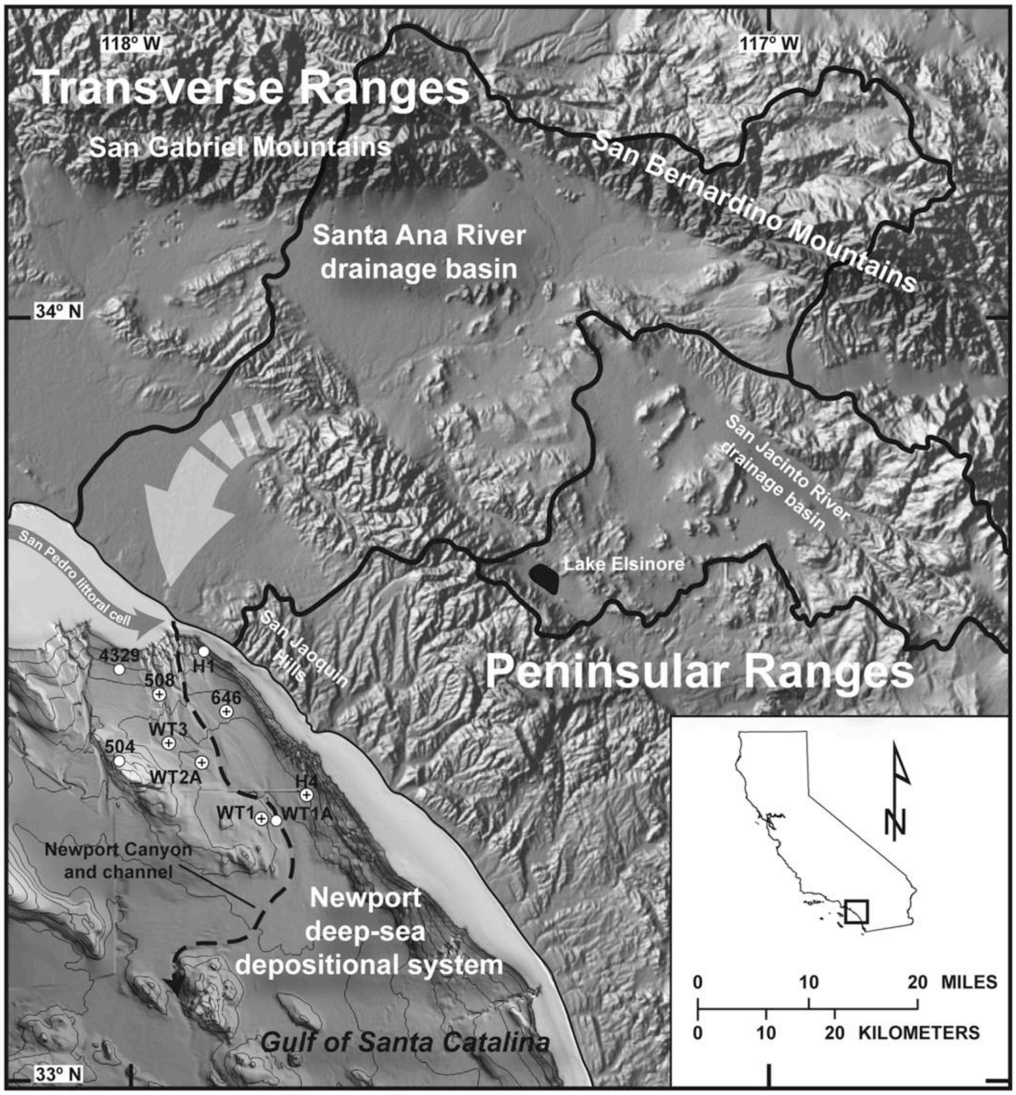

Figure 1. Southern California sediment-routing system of this study. Terrestrial segment includes the Santa Ana River drainage basin. The San Joaquin Hills, Lake Elsinore, and San Jacinto River drainage basins are identified. The submarine segment includes the San Pedro littoral cell and the Newport deep-sea depositional system. The offshore basin is the Gulf of Santa Catalina. The most recently active submarine conduit is highlighted with a dashed black line. Piston-core locations are white circles; cores used for deposition rates are identified with crosses. Submarine contour interval is 100 m. Base topography and bathymetry from GeoMapApp and Gardner and Dartnell (2002).

fluvial discharge in southern California (e.g., Inman and Jenkins 1999; Warrick and Milliman 2003); however, the twentieth century is an extremely small period of observation in the context of our Holocene study. Proxies indicate a wet early Holocene, followed by a long-term drying trend, which is attributed to changes in summer/winter insolation (Wells and Berger 1967; Kirby et al. 2005, 2007; fig. 2). Minimum winter and maximum summer insolation during the wet early Holocene increased the frequency of winter storms and enhanced the magnitude and spatial extent of the North American monsoon, the frequency of land-falling tropical cyclones, and the occurrence of regional convective storms (Kirby et al. 2007). The wet early Holocene is interpreted to have been effective at eroding and transporting sediment across the steep terrain of the San Jacinto River drainage basin to Lake Elsinore (Kirby et al. 2007). By extension, we posit that these wet conditions in southern California facilitated the transfer of sediment through other drainages, including the Santa Ana River drainage that

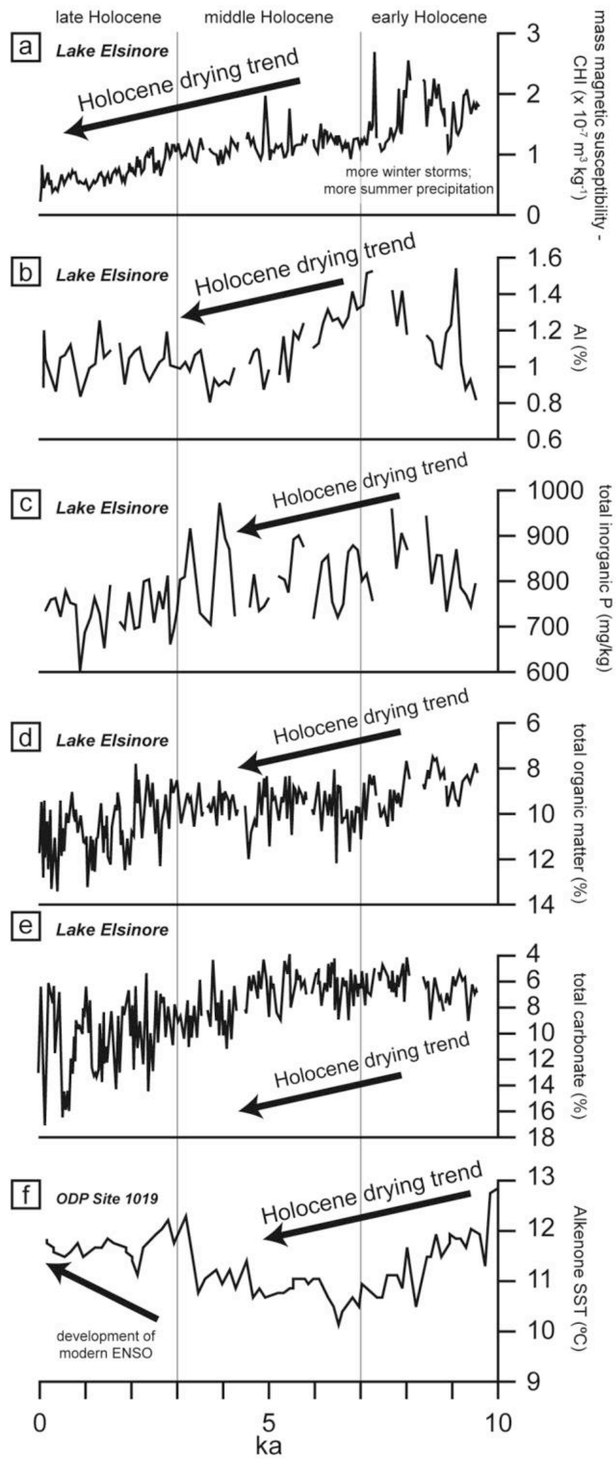

Figure 2. California climate proxies. *a–e*, Proxies from Lake Elsinore from Kirby et al. (2007). *f*, Alkenone sea surface temperature (SST) from Ocean Drilling Program (ODP) site 1019 (Barron et al. 2003). ENSO = El Niño–Southern Oscillation.

feeds the Newport deep-sea depositional system (Kirby et al. 2007). This inference is supported by Inman and Jenkins (1999), who show a strong positive relationship between precipitation and river sediment flux over the twentieth century in southern California.

Marine and terrestrial-derived climate proxies (diatoms, alkenones, pollen, $CaCO_3$ percentage, and total organic carbon) from Ocean Drilling Program (ODP) site 1019 offshore northern California (41.682°N, 124.930°W, 980 m bpsl) document a 100-yr resolution climatic evolution of coastal California since 16 ka (Barron et al. 2003; fig. 2). Similar to the Lake Elsinore record, ODP site 1019 reflects a wet early Holocene, followed by a drying trend through the middle Holocene (11.6–3.2 ka). However, during the late Holocene, after 3.2 ka, a permanent ~1°C increase in alkenone sea surface temperature (SST) signaled a warming of fall and winter SSTs (Barron et al. 2003; fig. 2). Contemporaneous terrestrial-derived pine pollen alternating with more alder and redwood pollen indicate rapid changes in moisture and seasonal temperature and are evidence for increased magnitude and frequency of El Niño–Southern Oscillation cycles (Barron et al. 2003; for interpretations of enhanced ENSO in the southwestern United States and southern California, see also Piechota et al. 1997; Cayan et al. 1999; Kirby et al. 2005; Masters 2006). The ENSO cycle is the major source of annual-to-decadal climate variability worldwide, and the coast of California is especially sensitive to ENSO phase (Masters 2006). During El Niño events, winter storms come from the west and strike California directly with strong winds and high waves, and as a result, precipitation and fluvial discharge are increased in southern California (Philander 1990; Masters 2006).

Data and Methods

For comparison with the terrestrial record, ground-truth data were obtained for the Newport deep-sea depositional system in the form of lithologies and 32 radiocarbon ages determined from 10 piston cores (<5 m below seafloor) collected during U.S. Geological Survey cruises O-2–99-SC and A-1-03-SC (U.S. Geological Survey 1999, 2003; figs. 1, 3). Cores were collected from different subenvironments of the Newport system, including canyon, channel, overbank, and splay elements (Normark et al. 1993; Posamentier and Kolla 2003), and described at centimeter-scale resolution (figs. 1, 3).

Sediment samples were dated by accelerator mass spectrometry (AMS) ^{14}C using foraminifera.

Table 1 gives both reservoir-corrected and calibrated ages. We determined that the highest degree of precision possible by AMS dating, provided by monospecific samples of the planktic foraminiferal species *Neogloboquadrina pachyderma*, was not necessary; therefore, the most abundant foraminiferal species in each sample were utilized instead. As a result, radiocarbon dates were determined using a mixed planktic foraminiferal assemblage (mostly *N. pachyderma*, *Neogloboquadrina dutertrei*, and *Globigerina bulloides*), *N. pachyderma* by itself, a mixed benthic foraminiferal assemblage, or monospecific samples of the benthic foraminiferal species *Uvigerina peregrina*, *Uvigerina juncea*, or *Gyroidina altiformis*.

Radiocarbon dating was provided by the National Ocean Sciences AMS (NOSAMS) Facility at the Woods Hole Oceanographic Institution. Ages were calculated using the accepted half-life of ^{14}C of 5568 yr (Stuiver and Polach 1977). The original measurements were obtained by a $^{14}C/^{12}C$ ratio that was corrected for isotope fractionation by normalizing for $\delta^{13}C$ by NOSAMS. Raw radiocarbon ages were then converted to calibrated ages using the CALIB program, version 5.0.1 (Stuiver and Reimer 1993). A reservoir age of 1750 yr was chosen for the benthic foraminiferal samples (Mix et al. 1999). An 800-yr reservoir age was used for the planktic foraminiferal samples with radiocarbon ages <12,000 yr (Southon et al. 1990; Kienast and McKay 2001), and a 1100-yr reservoir age was used for those >12,100 yr old (Kovanen and Easterbrook 2002). Calibrated ages were used in this study. Calibrated ages were <16 ka, with the majority <10 ka (table 1).

Holocene and latest Pleistocene deposition rates were measured between calibrated radiocarbon samples from six cores, each with more than three radiocarbon ages (cores 508, WT1, WT2A, WT3, H4, 646; fig. 4*a*; tables 1, 2). Normalized deposition rates are shown in figure 4*b* in order to highlight similar relative variability in rates between cores from different subenvironments of the Newport system. Therefore, variability in average rates for 1-k.yr. intervals from these six cores generally represents the depositional trends of the Newport Fan (fig. 5*a*; table 3). Average rates were calculated since 10 ka for comparison to various Holocene climate proxies (fig. 5*a*; table 3). The 10-ka limit on deposition rates was chosen because of the larger number of calibrated ages <10 ka and because comparative paleoclimate studies are predominantly focused on the Holocene (e.g., Kirby et al. 2007).

Southern California Sediment Routing and Deposition

Piston cores predominantly include abundant organic material and exhibit a range of grain sizes from mud to very fine-grained sand, with local coarser-grained sand and pebble-sized mud balls (fig. 3). Silt- and sand-rich beds exhibit subtle normal grading and local traction structures (i.e., plane and ripple laminae; fig. 3). Muddy, featureless beds are interpreted to be deposits of hemipelagic mud out of suspension (Stow and Piper 1984). Coarser-grained beds are interpreted to be the deposits of sediment gravity flows (Bouma 1962; Lowe 1982).

A piston core from the axis of the Newport channel, at ~720 m bpsl (WT1A), is relatively short (30 cm), presumably as a result of limited penetrability through the coarse-grained, channel floor substrate (figs. 1, 3). Similar to all the cores described in this study, core WT1A includes interbedded hemipelagic mud and turbidite sand. A radiocarbon age at the base of the core is 667 yr BP (table 1), which indicates that the Newport channel was active during the present highstand of sea level since the Last Glacial Maximum (LGM) at ~20 ka (Lambeck and Chappell 2001; Normark et al. 2009).

Holocene and latest Pleistocene deposition rates between radiocarbon samples range from ~8 to 133 cm/k.yr. (fig. 4*a*; table 2). Average deposition rates for 1-k.yr. intervals since 10 ka range from ~20 to 28 cm/k.yr. (fig. 5*a*; table 3). Deposition rates were similarly large during the latest Pleistocene to early Holocene transitional period (>7 ka) and a period during the latest Holocene (<3 ka; figs. 4, 5*a*). Deposition rates were smallest during the middle Holocene period from 7 to 3 ka (figs. 4, 5*a*). These depositional trends occurred during a period of rapid sea level rise between the LGM at ~20 ka and stillstand after ~6 ka (Lambeck and Chappell 2001; fig. 5). Pre-Holocene deposition rates were not calculated at 1-k.yr. intervals for analysis; however, visual inspection of sediment thicknesses and ages for the cores WT2A, WT3, and 646 (fig. 3), which include ages >10 ka, and consultation of table 2 suggests that rates were relatively large (e.g., as large as 133 cm/k.yr. from 12.90 to 13.05 ka in core 646).

Discussion: Highstand Fan Deposition and Climatic Signal Propagation

Variability in Holocene deposition rates on Newport Fan is similar to contemporaneous variability in proxy measurements of California climate (e.g.,

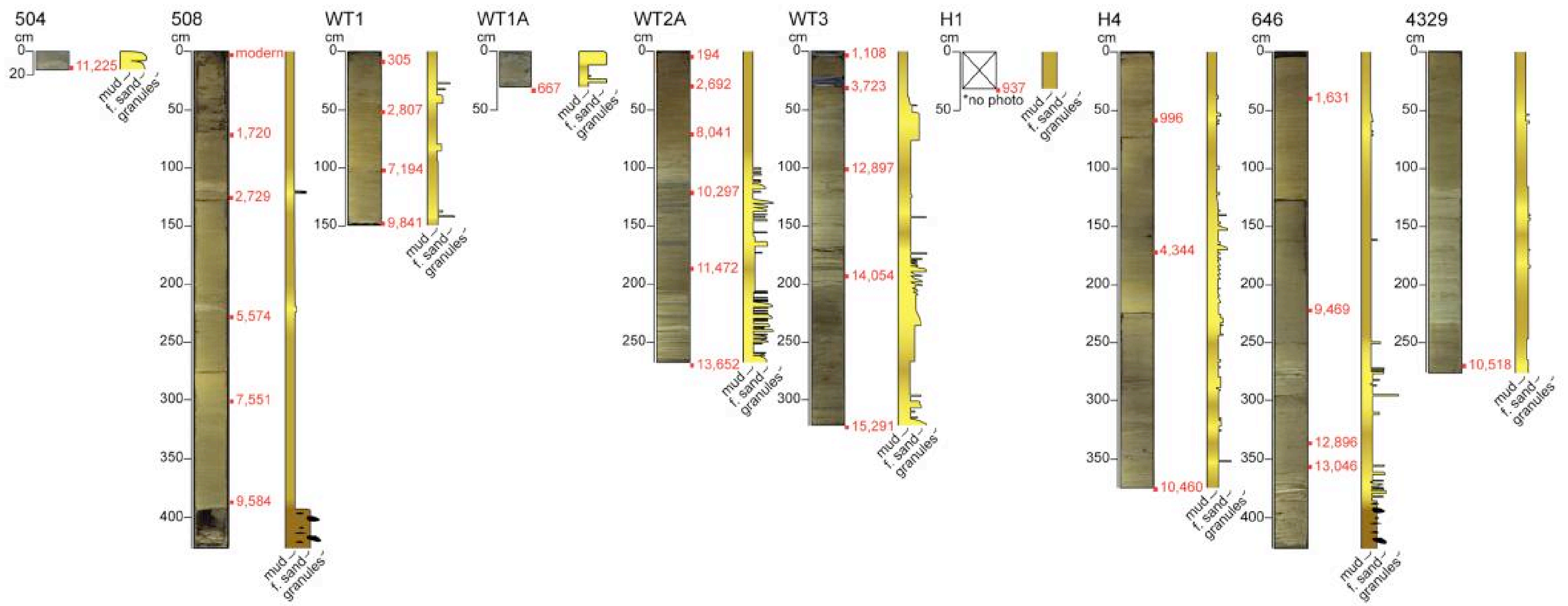

Figure 3. Photographs of piston cores, radiocarbon sample locations (*red boxes*), calibrated calendar ages (yr BP; *red text*), and grain-size profiles. Brown shading in grain-size profiles represents finer-grained sections; yellow shading represents coarse-grained turbidite sections.

Table 1. Gulf of Santa Catalina Radiocarbon Ages

Piston core	Sample depth (m below present sea level)	Description	$\delta^{13}C$	Age (yr)	Age error (yr)	Corrected reservoir age (yr)	Calendar age (yr BP)
504	.13–.15	Mixed benthic foraminifera	.23	11,600	±45	9,850	11,225
508	.03–.05	Mixed benthic foraminifera	−.58	1,060	±25	(−690)	Too young
508	.70–.72	Mixed planktic foraminifera	1.17	2,530	±30	1,730	1,720
508	1.25–1.27	Mixed benthic foraminifera	−.52	4,300	±35	2,550	2,729
508	2.28–2.30	Mixed benthic foraminifera	.65	6,560	±40	4,810	5,574
508	3.00–3.02	Mixed benthic foraminifera	−.62	8,420	±60	6,670	7,551
508	3.86–3.88	*Neogloboquadrina pachyderma*	.38	9,320	±60	8,520	9,584
WT1	.10–.12	Mixed benthic foraminifera	−.85	2,010	±30	260	305
WT1	.50–.52	Mixed benthic foraminifera	−.78	4,390	±40	2,640	2,807
WT1	1.00–1.02	Mixed benthic foraminifera	−.90	8,010	±50	6,260	7,194
WT1	1.48–1.49	Mixed benthic foraminifera	−1.47	10,450	±50	8,700	9,841
WT1A	.30–.40	Mixed benthic foraminifera	−.89	2,460	±35	710	667
WT2A	.04–.06	Mixed benthic foraminifera	−.67	1,910	±35	160	194
WT2A	.30–.32	Mixed benthic foraminifera	−.7	4,250	±30	2,500	2,692
WT2A	.70–.72	Mixed benthic foraminifera	−.92	8,930	±50	7,180	8,041
WT2A	1.20–1.22	Mixed benthic foraminifera	−1.14	10,800	±40	9,050	10,297
WT2A	1.86–1.89	Mixed benthic foraminifera	−1.22	11,750	±60	10,000	11,472
WT2A	2.67–2.79	*Uvigerina juncea*	−1.42	13,550	±80	11,800	13,652
WT3	.06–.08	Mixed benthic foraminifera	−.71	2,900	±40	1,150	1,108
WT3	.30–.32	Mixed benthic foraminifera	−.80	5,130	±40	3,380	3,723
WT3	1.01–1.03	Mixed benthic foraminifera	−1.19	12,700	±65	10,950	12,897
WT3	1.93–1.95	Mixed benthic foraminifera	−2.17	13,950	±65	12,200	14,054
WT3	3.21–3.34	*Gyroidina altiformis*	−1.43	14,700	±85	12,950	15,291
H1	.30–.38	Mixed benthic foraminifera	−.04	2,740	±30	990	937
H4	.60–.62	Mixed benthic foraminifera	−1.66	2,800	±40	1,050	996
H4	1.73–1.75	Mixed benthic foraminifera	−1	5,590	±40	3,840	4,344
H4	3.74–3.84	Mixed benthic foraminifera	−2.35	10,950	±65	9,200	10,460
646	.40–.42	Mixed benthic foraminifera	−.68	3,410	±35	1,660	1,631
646	2.25–2.27	Mixed benthic foraminifera	−1.09	10,150	±50	8,400	9,469
646	3.37–3.39	*Uvigerina peregrina*	−1.08	12,700	±60	10,950	12,896
646	3.56–3.58	*U. peregrina*	−1.15	12,900	±50	11,150	13,046
4329	2.69–2.71	Mixed benthic foraminifera	−.39	11,000	±45	9,250	10,518

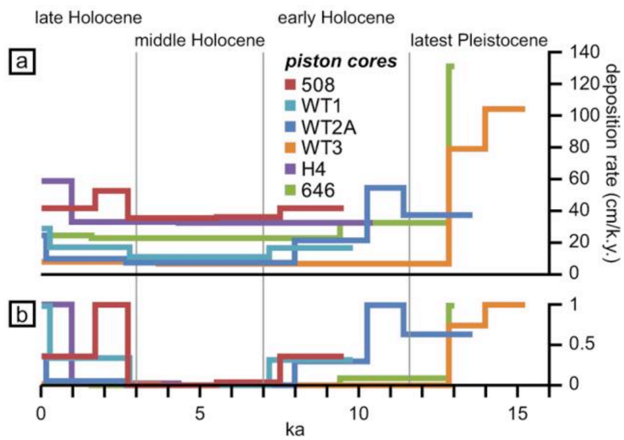

Figure 4. Holocene Newport Fan deposition. *a*, Holocene and latest Pleistocene deposition rates. *b*, Normalized deposition rates from *a*.

Barron et al. 2003; Kirby et al. 2007; fig 5). Larger deposition rates during the early Holocene (>7 ka) correspond with a wetter climate, which resulted in increased discharge of water and sediment from southern California rivers (Barron et al. 2003; Kirby et al. 2007; fig. 5). This increased discharge facilitated the delivery of sediment to the Newport deep-sea depositional system. Smaller deposition rates during the middle Holocene (7–3 ka) correspond with a drying trend (Barron et al. 2003; Kirby et al. 2007; fig. 5). Diminished precipitation appears to have inhibited the transfer of sediment from land to sea. Another possibility is that Holocene marine transgression temporarily disconnected the Newport Canyon from the Santa Ana River from ~7 to 3 ka. However, this possibility is unlikely as a result of evidence for continued turbidite deposition during this period, according to Newport deep-sea piston cores (fig. 3). During the late Holocene (<3 ka), more rapid deposition is likely a result of enhanced ENSO frequency and magnitude in southern California (Piechota et al. 1997; Cayan et al. 1999; Barron et al. 2003; Kirby et al. 2005; Masters 2006; fig. 5). Increased sediment flux from the Santa Ana River to the Newport deep-sea depositional system has been documented during twentieth-century ENSO conditions (Warrick and Milliman 2003). Climate proxies of Kirby et al. (2007) from Lake Elsinore lack evidence of late Holocene ENSO conditions (fig. 2). This omission might be because proxies from Lake Elsinore represent local climate variability relative to the deep-sea records, which are the manifestation of forcings that operated over an entire sediment-routing system, from terrestrial source areas to deep-sea sinks. In semiarid settings, like southern California, climatic variability can control terrestrial vegetation (Heusser 1978), which can also impact the transfer of sediment to deep-sea sites of deposition (Douglas 1967; Hooke 2000; Vanacker et al. 2007). However, the relatively steep topography of the tectonically active Santa Ana River drainage basin and strong positive relationship between Holocene climate proxies and deep-sea deposition suggests that the effects of vegetation on sediment storage and release are minor here, at least during the Holocene. Pre-Holocene climate data for comparison are generally lacking; however, it is possible that relatively large pre-Holocene rates are a result of lower sea level facilitating the activity of numerous deep-sea canyons and channels of the Newport system and adjacent slope, rather than just a single canyon and channel, such as during the Holocene marine transgression and highstand (cf. Posamentier et al. 1991).

Table 2. Holocene and Latest Pleistocene Newport Fan Deposition Rates between Radiocarbon Samples

	Section 1			Section 2			Section 3		
Piston core	Thickness (cm)	Interval (k.yr.)	Rate (cm/k.yr.)	Thickness (cm)	Interval (k.yr.)	Rate (cm/k.yr.)	Thickness (cm)	Interval (k.yr.)	Rate (cm/k.yr.)
508	72	0–1.72	41.86	53	1.72–2.73	52.53	102	2.73–5.57	35.85
WT1	9	0–.31	29.51	43	.31–2.81	17.19	50	2.81–7.19	11.40
WT2A	5	0–.19	25.77	25	.19–2.69	10.01	41	2.69–8.04	7.66
WT3	32	0–3.72	8.60	70	3.72–12.90	7.63	91	12.90–14.05	78.65
H4	59	0–1.00	59.24	113	1.00–4.34	33.75	202	4.34–10.46	33.03
646	41	0–1.63	25.14	180	1.63–9.47	22.97	113	9.47–12.90	32.97
	Section 4			Section 5			Section 6		
508	72	5.57–7.55	36.42	86	7.55–9.58	42.30			
WT1	45	7.19–9.84	17.00						
WT2A	50	8.04–10.30	22.16	64	10.30–11.47	54.47	82	11.47–13.65	37.61
WT3	129	14.05–15.29	104.28						
H4									
646	20	12.90–13.05	133.33						

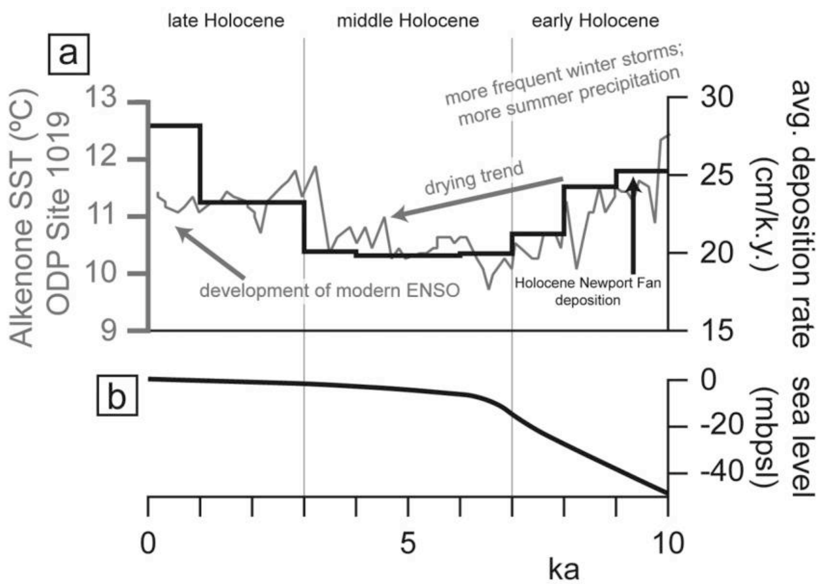

Figure 5. Holocene Newport Fan deposition and southern California climate. *a*, Average deposition rates for all six cores for 1-k.yr. intervals since 10 ka versus alkenone sea surface temperature (SST) from Ocean Drilling Program (ODP) site 1019 (*gray*; Barron et al. 2003). *b*, Sea level curve (Lambeck and Chappell 2001). A color version of this figure is available in the online edition of the *Journal of Geology*.

Here we demonstrate the utility of deep-sea turbidite depositional trends as paleoclimate proxies in a southern California source-to-sink sedimentary system, which might be useful in other spatially restricted settings.

"Reactive" versus "Buffered" Sediment-Routing Systems. Why are climatic signals rapidly propagated through the southern California sediment-routing system of this study, especially despite significant sea level change during the Holocene (~50 m since 10 ka; Lambeck and Chappell 2001; fig. 5*b*)? Recent studies of deep-sea deposition during sea level highstands, especially from spatially restricted sediment-routing systems in southern California, have demonstrated the importance of connectivity between terrestrial and submarine segments of routing systems (Covault et al. 2007; Normark et al. 2009; Romans et al. 2009). Offshore southern California, tectonic deformation creates steep slopes outboard of narrow shelves, and as a result, canyon-head incision across the shelf can keep pace with transgression of the shoreline (Normark et al. 2009). In this way, deep-sea conduits can maintain connections to nearby hinterland source areas and deliver sediment to fans regardless of sea level. As a result, terrestrial changes rapidly impact deposition in the deep sea. Allen (2008*b*) called such sediment-routing systems, that is, those in which the land- or seascape responds rapidly to a perturbation, "reactive." The Hueneme Fan, which is the submarine depositional component of a reactive southern California sediment-routing system analogous to the system of this study, also exhibits increased delivery of sediment to the deep sea in re-

Table 3. Average Deposition Rates for 1-k.yr. Intervals since 10 ka

Piston core	Rate (cm/k.yr.)									
	0–1 ka	1–2 ka	2–3 ka	3–4 ka	4–5 ka	5–6 ka	6–7 ka	7–8 ka	8–9 ka	9–10 ka
508	41.86	44.85	48.01	35.85	35.85	36.09	36.42	39.06	42.30	42.30
WT1	20.94	17.19	16.07	11.40	11.40	11.40	11.40	15.91	17.00	17.00
WT2A	13.07	10.01	9.29	7.66	7.66	7.66	7.66	7.66	21.57	22.16
WT3	8.60	8.60	8.60	8.33	7.63	7.63	7.63	7.63	7.63	7.63
H4	59.14	33.75	33.75	33.75	33.28	33.03	33.03	33.03	33.03	33.03
646	25.14	24.34	22.97	22.97	22.97	22.97	22.97	22.97	22.97	28.28
Average	28.12	23.12	23.11	19.99	19.80	19.80	19.85	21.04	24.08	25.07

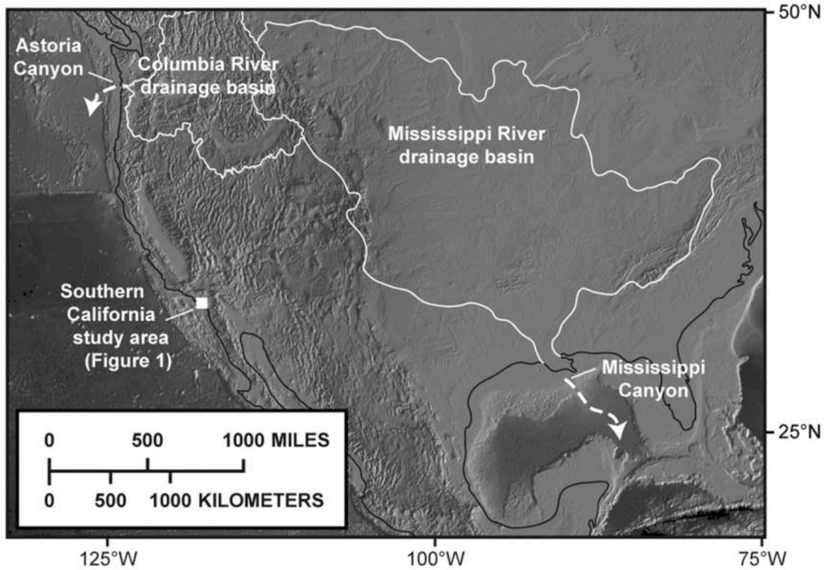

Figure 6. North America topography and nearshore bathymetry. Expansive Mississippi and Columbia river drainage basins are outlined with white lines. Offshore canyon-and-channel systems are white dashed lines. The relatively small southern California sediment-routing system of this study is highlighted with a white box. Base topography and bathymetry from GeoMapApp.

sponse to ENSO variability since ~3 ka (Romans et al. 2009).

In contrast, transient sediment storage in larger sediment-routing systems that drain entire continents can introduce significant lags between terrestrial climatic forcings and deep-sea deposition (Milliman and Syvitski 1992; Métivier and Gaudemer 1999; Castelltort and Van Den Dreissche 2003; Allen 2008*a*). Allen (2008*b*) called such systems "buffered." Figure 6 shows the Mississippi River drainage basin, which extends across the continental United States. The large size of the terrestrial segment of this sediment-routing system, including an extensive lowland flood plain, affords more opportunities for sediment to be sequestered in accommodation en route to the Mississippi Canyon relative to the much smaller southern California system of this study (fig. 6). The buffering timescale in such settings might exceed millions of years, and as a result, deep-sea records of perturbations and sediment flux from land to sea might be unrecognizable (Allen 2008*a*). It is important to note, however, that the Mississippi River delivered voluminous subglacial meltwater discharge and sediment to the submarine canyon and fan during marine transgression at least until ~12 or 11 ka (Kolla and Perlmutter 1993). But when the deep-sea segment of the Mississippi sediment-routing system shut down during the Holocene, sediment was predominantly retained in terrestrial and shallow-marine settings until the next sea level fall (Kolla and Perlmutter 1993).

As we alluded to in the discussion of the Mississippi system, not all large sediment-routing systems are continuously buffered. For example, large high-latitude systems are sensitive to climatic variability associated with glacial-to-interglacial transitions, during which catastrophic floods can rapidly transport sediment thousands of kilometers from source to sink (Brunner et al. 1999; Zuffa et al. 2000; Normark and Reid 2003; Piper and Normark 2009). Figure 6 shows the relatively large Columbia River drainage basin, which fed sediment to the Astoria Canyon during the Lake Missoula and other latest Pleistocene floods (Normark and Reid 2003). Radiocarbon age dates from ODP sites 1037 and 1038, which are >1000 km from the Columbia River mouth along a deep-sea conduit, corroborate the synchronicity of deep-sea deposition and terrestrial flooding (Brunner et al. 1999; Zuffa et al. 2000). Similar to the smaller southern California sediment-routing system of this study, the Columbia River–to-Astoria deep-sea depositional system is, at least temporarily, reactive. That is to say, the sedimentary processes inherent to high-latitude systems (i.e., extreme sensitivity to subglacial conditions) temporarily facilitate relatively efficient sediment flux to the deep sea (cf. the Laurentian Channel and other high-latitude systems of the eastern Canadian margin; Piper and Normark 2009). Therefore, such reactive sediment-routing systems, both large and small, can at least temporarily rapidly propagate climate and sediment-flux signals, and as a result, changes in the rates and character of deep-sea deposition might faithfully reflect terrestrial climatic fluctuations.

Conclusions

We employ an integrated piston-core and radiocarbon-age data set from the Newport deep-sea depositional system, and on- and offshore California climate proxies, in order to test the hypothesis that climatic signals are rapidly propagated from source to sink in a spatially restricted, consistently linked sediment-routing system. Variability in Holocene Newport deep-sea fan deposition rates is related to contemporaneous variability in proxy measurements of California climate: larger deposition rates during the early and late Holocene epoch correspond with increased precipitation and complex ocean-atmosphere interactions, which promoted rapid funneling of sediment through the routing system. This relationship is evident because, unlike many sediment-routing systems, the Newport submarine canyon-and-channel system was consistently linked to the Santa Ana River, which promoted sediment delivery in spite of evidence of significant sea level rise (~50 m; Lambeck and Chappell 2001). The efficiency of sediment transport and delivery in this southern California routing system indicates that, in reactive systems, deep-sea fan deposition can be useful in the assessment of past climate.

ACKNOWLEDGMENTS

J. A. Covault, B. W. Romans, and A. Fildani thank the Clastic Stratigraphy R & D team at Chevron Energy Technology Company, and especially M. Sullivan, for encouraging such holistic research on sedimentary systems and B. Ritts for providing a thorough review of this manuscript. J. A. Covault thanks B. Morris and J. Ericsson at ConocoPhillips for support during piston-core description and G. E. Hilley for insightful discussions. We thank the ships, crew, and scientific parties of U.S. Geological Survey cruises O-2-99-SC and A-1-03-SC. We also thank B. Normark for his mentorship and inspiration. We thank three anonymous reviewers for their constructive comments. J. A. Covault dedicates this work to Katherine and Orion Covault, whose labor and arrival, respectively, allowed for this study to be completed.

REFERENCES CITED

Allen, P. A. 1997. Earth surface processes. Oxford, Blackwell Science, 404 p.

———. 2007. Earth science: sediment en route to oblivion. Nature 450:490–491.

———. 2008*a*. From landscapes into geological history. Nature 451:274–276.

———. 2008*b*. Time scales of tectonic landscapes and their sediment routing systems. Geol. Soc. Lond. Spec. Publ. 296:7–28.

Barron, J. A.; Heusser, L.; Herbert, T.; and Lyle, M. 2003. High-resolution climatic evolution of coastal northern California during the past 16,000 years. Paleoceanography 18:1020, doi:10.1029/2002PA000768.

Bouma, A. H. 1962. Sedimentology of some flysch deposits. Amsterdam, Elsevier, 168 p.

Brunner, C. A.; Normark, W. R.; Zuffa, G. G.; and Serra, F. 1999. Deep-sea sedimentary record from the late Wisconsin cataclysmic floods from the Columbia River. Geology 27:463–466.

Castelltort, S., and Van Den Dreissche, J. 2003. How plausible are high-frequency sediment supply-driven cycles in the stratigraphic record? Sediment. Geol. 157: 3–13.

Cayan, D. R.; Redmond, K. T.; and Riddle, L. G. 1999. ENSO and hydrologic extremes in the western United States. J. Clim. 12:2881–2893.

Covault, J. A.; Normark, W. R.; Romans, B. W.; and Graham, S. A. 2007. Highstand fans in the California borderland: the overlooked deep-water depositional systems. Geology 35:783–786.

Douglas, J. 1967. Man, vegetation and the sediment yield of rivers. Nature 215:925–928.

Einsele, G.; Chough, S. K.; and Shiki, T. 1996. Depositional events and their records: an introduction. Sediment. Geol. 104:1–9.

Figueiredo, J.; Hoom, C.; van der Ven, P.; and Soares, E. 2009. Late Miocene onset of the Amazon River and the Amazon deep-sea fan: evidence from the Foz do Amazon Basin. Geology 37:619–622.

Gardner, J. V., and Dartnell, P. 2002. Multibeam mapping of the Los Angeles, California margin. U.S. Geol. Surv. Open-File Rep. 02–162, http://geopubs.wr.usgs.gov/open-file/of02−162/.

Heusser, L. 1978. Pollen in Santa Barbara Basin: a 12,000-yr record. Geol. Soc. Am. Bull. 89:673–678.

Hooke, R. L. 2000. Toward a uniform theory of clastic sediment yield in fluvial systems. Geol. Soc. Am. Bull. 112:1778–1786.

Inman, D. L., and Jenkins, S. A. 1999. Climate change and the episodicity of sediment flux of small California rivers. J. Geol. 107:251–270.

Kienast, S. S., and McKay, J. L. 2001. Sea surface tem-

peratures in the subarctic northeast Pacific reflect millennial-scale climate oscillations during the last 16 kyrs. Geophys. Res. Lett. 28:1563–1566.
Kirby, M. E.; Lund, S. P.; Anderson, M. A.; and Bird, B. W. 2007. Insolation forcing of Holocene climate change in Southern California: a sediment study from Lake Elsinore. J. Paleolimnol. 38:395–417.
Kirby, M. E.; Lund, S. P.; and Poulsen, C. J. 2005. Hydrologic variability and the onset of modern El Niño-Southern Oscillation: a 19,250-year record from Lake Elsinore, southern California. J. Quat. Sci. 20:239–254.
Kirby, M. E.; Poulsen, S. P.; Lund, S. P.; Patterson, W. P.; Reidy, L.; and Hammond, D. E. 2004. Late Holocene lake-level dynamics inferred from magnetic susceptibility and stable oxygen isotope data: Lake Elsinore, Southern California. J. Paleolimnol. 31:275–293.
Kolla, V., and Perlmutter, M. A. 1993. Timing of turbidite sedimentation on the Mississippi Fan. AAPG Bull. 77: 1129–1141.
Kovanen, D. J., and Easterbrook, D. J. 2002. Paleodeviations of radiocarbon marine reservoir values for the northeast Pacific. Geology 30:243–246.
Lambeck, K., and Chappell, J. 2001. Sea level change through the last glacial cycle. Science 292:679–686.
Lowe, D. R. 1982. Sediment gravity flows. II. Depositional models with special reference to the deposits of high-density turbidity currents. J. Sediment. Petrol. 52:279–297.
Masters, P. M. 2006. Holocene sand beaches of southern California: ENSO forcing and coastal processes on millennial scales. Palaeogeogr. Palaeoclimatol. Palaeoecol. 232:73–95.
Menard, H. W. 1955. Deep-sea channels, topography, and sedimentation. AAPG Bulletin 39:236–255.
Métivier, F., and Gaudemer, Y. 1999. Stability of output fluxes of large rivers in South and East Asia during the last 2 million years: implications for floodplain processes. Basin Res. 11:293–304.
Milliman, J. D., and Syvitski, J. P. M. 1992. Geomorphic/tectonic control of sediment discharge to the ocean: the importance of small mountainous rivers. J. Geol. 100:525–544.
Mix, A. C.; Lund, D. C.; Pisias, N. G.; and Bodén, P. 1999. Rapid climate oscillations in the northeast Pacific during the last deglaciation reflect Northern and Southern Hemisphere sources. *In* Clark, P.; Webb, R. S.; and Keigwin, L. D., eds. Mechanisms for global climate change at millennial time scales. Geophysical Monograph Series 112. Washington, DC, American Geophysical Union, p. 127–148.
Normark, W. R. 1970. Growth patterns of deep-sea fans. AAPG Bull. 54:2170–2195.
Normark, W. R.; Piper, D. J. W.; Romans, B. W.; Covault, J. A.; Dartnell, P.; and Sliter, R. 2009. Submarine canyon and fan systems of the California continental borderland. *In* Lee, H. J., and Normark, W. R., eds. Earth science in the urban ocean: the southern California continental borderland. Geol. Soc. Am. Spec. Pap. 454, p. 141–168.
Normark, W. R.; Posamentier, H.; and Mutti, E. 1993. Turbidite systems: state of the art and future directions. Rev. Geophys. 31:91–116.
Normark, W. R., and Reid, J. A. 2003. Extensive deposits on the Pacific plate from Late Pleistocene North American glacial lake outbursts. J. Geol. 111:617–637.
Philander, S. G. 1990. El Niño, La Niña, and the Southern Oscillation. San Diego, CA, Academic Press, 289 p.
Piechota, T. C.; Dracup, J. A.; and Fovell, R. G. 1997. Western US streamflow and atmospheric circulation patterns during El Niño-Southern Oscillation. J. Hydrol. 201:249–271.
Piper, D. J. W., and Normark, W. R. 2001. Sandy fans: from Amazon to Hueneme and beyond. AAPG Bull. 85:1407–1438.
———. 2009. Processes that initiate turbidity currents and their influence on turbidites: a marine geology perspective. J. Sediment. Res. 79:347–362.
Posamentier, H. W.; Erskine, R. D.; and Mitchum, Jr., R. M. 1991. Submarine fan deposition within a sequence stratigraphic framework. *In* Weimer, P., and Link, M. H., eds. Seismic facies and sedimentary processes of submarine fans and turbidite systems. New York, Springer, p. 127–136.
Posamentier, H. W., and Kolla, V. 2003. Seismic geomorphology and stratigraphy of depositional elements in deep-water settings. J. Sediment. Res. 73:367–388.
Romans, B. W.; Normark, W. R.; McGann, M. M.; Covault, J. A.; and Graham, S. A. 2009. Coarse-grained sediment delivery and distribution in the Holocene Santa Monica Basin, California: implications for evaluating source-to-sink flux at millennial time scales. Geol. Soc. Am. Bull. 121:1394–1408, doi:10.1130/B26393.1.
Ryan, H. F.; Legg, M. R.; Conrad, J. E.; and Sliter, R. 2009. Recent faulting in the Gulf of Santa Catalina: San Diego to Dana Point. *In* Lee, H. J., and Normark, W. R., eds. Earth science in the urban ocean: the southern California continental borderland. Geol. Soc. Am. Spec. Pap. 454, p. 291–315.
Shepard, F. P., and Emery, K. O. 1941. Submarine topography off the California coast: canyon and tectonic interpretation. Geol. Soc. Am. Spec. Pap. 31, 171 p.
Southon, J. R.; Nelson, D. E.; and Vogel, J. S. 1990. A record of past ocean-and-atmosphere radiocarbon differences from the northeast Pacific. Paleoceanography 5:197–206.
Stokstad, E. 2001. Myriad ways to reconstruct past climate. Science 292:658–659.
Stow, D. A. V., and Piper, D. J. W., eds. 1984. Fine-grained sediment: deep-water processes and facies. Geol. Soc. Lond. Spec. Publ. 15, 646 p.
Stuiver, M., and Polach, H. A. 1977. Discussion: reporting of ^{14}C data. Radiocarbon 19:355–363.
Stuiver, M., and Reimer, P. J. 1993. Extended ^{14}C data base and revised CALIB 3.0 ^{14}C age calibration program. Radiocarbon 35:215–230.
U.S. Geological Survey. 1999. Coastal and Marine Geology InfoBank. CMG O-2-99-SC metadata, http://walrus.wr.usgs.gov/infobank/o/o299sc/html/o-2-99-sc.meta.html.

———. 2003. Coastal and Marine Geology InfoBank. CMG A-1-03-SC metadata, http://walrus.wr.usgs.gov/infobank/a/a103sc/html/a-1-03-sc.meta.html.

Vanacker, V.; von Blackenburg, F.; Govers, G.; Molina, A.; Poesen, J.; Deckers, J.; and Kubik, P. 2007. Restoring dense vegetation can slow mountain erosion to near natural benchmark levels. Geology 35:303–306.

Verschuren, D. 2003. Lake-based climate reconstruction in Africa: progress and challenges. Hydrobiologia 500: 315–330.

Warrick, J. A., and Milliman, J. D. 2003. Hyperpycnal sediment discharge from semiarid southern California rivers: implications for coastal sediment budgets. Geology 31:781–784.

Wells, P. V., and Berger, R. 1967. Late Pleistocene history of coniferous woodland in the Mohave Desert. Science 155:1640–1647.

Zuffa, G. G.; Normark, W. R.; Serra, F.; and Brunner, C. A. 2000. Turbidite megabeds in an oceanic rift valley recording Jökulhlaups of Late Pleistocene glacial lakes of the western United States. J. Geol. 108:253–274.